



**HAL**  
open science

## Hurricanes as unstable fixed points of the tropical atmospheric dynamics

Davide Faranda, Gabriele Messori, Pascal Yiou, Soulivanh Thao, Flavio Pons,  
Berengere Dubrulle

► **To cite this version:**

Davide Faranda, Gabriele Messori, Pascal Yiou, Soulivanh Thao, Flavio Pons, et al.. Hurricanes as unstable fixed points of the tropical atmospheric dynamics. 2022. hal-03219409v2

**HAL Id: hal-03219409**

**<https://hal.science/hal-03219409v2>**

Preprint submitted on 30 Mar 2022 (v2), last revised 7 Dec 2022 (v4)

**HAL** is a multi-disciplinary open access archive for the deposit and dissemination of scientific research documents, whether they are published or not. The documents may come from teaching and research institutions in France or abroad, or from public or private research centers.

L'archive ouverte pluridisciplinaire **HAL**, est destinée au dépôt et à la diffusion de documents scientifiques de niveau recherche, publiés ou non, émanant des établissements d'enseignement et de recherche français ou étrangers, des laboratoires publics ou privés.

# 1 Hurricanes as unstable fixed points of the tropical atmospheric dynamics

2 D. Faranda,<sup>1,2,3, a)</sup> G. Messori,<sup>4,5</sup> P. Yiou,<sup>1</sup> S. Thao,<sup>1</sup> F. Pons,<sup>1</sup> and B. Dubrulle<sup>6</sup>

3 <sup>1)</sup>*Laboratoire des Sciences du Climat et de l'Environnement,*

4 *UMR 8212 CEA-CNRS-UVSQ, Université Paris-Saclay & IPSL,*

5 *CE Saclay l'Orme des Merisiers, 91191, Gif-sur-Yvette, France*

6 <sup>2)</sup>*London Mathematical Laboratory, 8 Margravine Gardens, London, W6 8RH,*

7 *UK*

8 <sup>3)</sup>*LMD/IPSL, Ecole Normale Supérieure, PSL research University, 75005, Paris,*

9 *France*

10 <sup>4)</sup>*Department of Earth Sciences and Centre of Natural Hazards*

11 *and Disaster Science (CNDS), Uppsala University, Uppsala,*

12 *Sweden*

13 <sup>5)</sup>*Department of Meteorology and Bolin Centre for Climate Research,*

14 *Stockholm University, Stockholm, Sweden.*

15 <sup>6)</sup>*SPEC, CEA, CNRS, Université Paris-Saclay, F-91191 CEA Saclay, Gif-sur-Yvette,*

16 *France.*

17 (Dated: 30 March 2022)

18 Hurricanes — and more broadly tropical cyclones — are high-impact weather phenom-  
19 ena whose adverse socio-economic and ecosystem impacts affect a considerable part of  
20 the global population. Despite having a reasonably robust meteorological understanding  
21 of tropical cyclones, their simulation in numerical models remains challenging. Conse-  
22 quently, future changes in the frequency of occurrence and intensity of tropical cyclones  
23 are still debated. Here, we diagnose possible reasons for the poor representation of tropical  
24 cyclones in numerical models, by considering the cyclones as chaotic dynamical systems.  
25 We follow 197 tropical cyclones which occurred between 2010 and 2020 in the North At-  
26 lantic using the HURDAT2 and ERA5 datasets. We measure the cyclones' instantaneous  
27 number of active degrees of freedom (local dimension) and the persistence of their sea-level  
28 pressure and potential vorticity fields. During the most intense phases of the cyclones, and  
29 specifically when cyclones reach hurricane strength, there is a collapse of degrees of free-  
30 dom and an increase in persistence, hinting to the existence of an unstable fixed point of  
31 the dynamics. Hurricanes may thus be interpreted as unstable fixed points of rotational  
32 energy, and their evolution is well-captured by the potential vorticity map of the cyclone  
33 eye. In analogy with high-dissipation intermittent events in turbulent flows, this suggests  
34 strategies to improve numerical simulations of intense tropical cyclones, and specifically  
35 the need for adaptive parametrisation schemes.

---

<sup>a)</sup>Correspondence to [davide.faranda@lscce.ipsl.fr](mailto:davide.faranda@lscce.ipsl.fr)

## 36 I. LEAD PARAGRAPH

37 **Tropical cyclones are both high-impact weather events and challenging phenomena from**  
38 **the point of view of numerical modelling. While their lifecycle is relatively well understood,**  
39 **there are still difficulties in the representation of their dynamics in weather and climate**  
40 **models, and in drawing robust conclusions on how different climate conditions may affect**  
41 **their frequency of occurrence and intensity. Here, we consider tropical cyclones as chaotic**  
42 **dynamical systems. We show that the formation of particularly intense cyclones, termed**  
43 **hurricanes in the North Atlantic, coincides with a reduction of the phase space of the atmo-**  
44 **spheric dynamics to a low-dimensional object, where few rotational kinetic degrees of free-**  
45 **dom dominate the dynamics. This behavior, also encountered in laboratory turbulent flows**  
46 **near strongly dissipative structures, is typical of unstable fixed points of high-dimensional**  
47 **dynamical systems. This analogy suggests the need for adaptive parameterisations to inte-**  
48 **grate the governing equations when simulating intense tropical cyclones in numerical climate**  
49 **models.**

## 50 II. INTRODUCTION

51 Tropical cyclones are high-impact extreme weather events. For example, they are the costli-  
52 est natural disaster category in the United States<sup>1,2</sup>, with the damage related to hurricane Katrina  
53 (2005) alone amounting to about 1% of the gross domestic product of the country<sup>2</sup>. Trends in  
54 the frequency of occurrence and intensity of tropical cyclones are difficult to discern in observa-  
55 tions because of their relative rarity and of the brevity of highly spatially and temporally resolved  
56 datasets, which rely on satellite observations<sup>3</sup>. Projections of future climates indicate an increase  
57 in the intensity of tropical cyclones in the North Atlantic sector, albeit only with medium confi-  
58 dence<sup>4</sup> as reproducing the dynamics of the most severe events is difficult even in the most advanced  
59 global or regional climate models<sup>5</sup>. Indeed, while mid-latitude synoptic dynamics mostly origi-  
60 nate from the chaotic structure of the motions associated with baroclinic instability<sup>6,7</sup>, tropical  
61 cyclones are characterized by a rapid organization of convectively unstable flows whose dynamics  
62 is turbulent and highly sensitive to boundary conditions<sup>8</sup>. To understand the reasons for the poor  
63 representation of tropical cyclones in numerical models, we adopt a dynamical system methodol-  
64 ogy which represents the cyclones as states of a chaotic, high-dimensional system. We specifically

65 compute two metrics reflecting instantaneous properties of the cyclones, namely persistence and  
66 local dimension. Local dimension is a proxy for the system’s number of active degrees of free-  
67 dom, and can be linked to the system’s predictability<sup>9–11</sup>. Persistence provides information about  
68 the dominant time scale of the dynamics. Both metrics may easily be applied to large datasets,  
69 such as climate reanalyses. They have recently provided insights on a number of geophysical  
70 phenomena, including transitions between transient metastable states of the mid-latitude atmo-  
71 sphere<sup>9,12</sup>, palaeoclimate attractors<sup>13,14</sup>, slow earthquake dynamics<sup>15</sup> and changes in mid-latitude  
72 atmospheric predictability under global warming<sup>16</sup>.

73 All these applications have taken an Eulerian point-of-view, focusing on a fixed spatio-temporal  
74 domain. Here, we provide the first application of the two metrics from a (semi)-Lagrangian per-  
75 spective, by computing the persistence and local dimension of tropical cyclones which we track in  
76 space and time. This approach is particularly suited to study the complex behavior of convectively  
77 unstable flow systems<sup>17,18</sup>. Our aim is to understand whether tropical cyclones — and especially  
78 the most intense ones — have an underlying structure similar to a generic point of the phase space  
79 or whether their dynamics has peculiar specificities. The first case would imply that numerical  
80 parametrizations developed for generic tropical climate states should work well when applied to  
81 small-scale features of tropical cyclones. The second case would imply that cyclones are unstable  
82 fixed points of the phase space, thus leading to the conclusion that parametrizations designed for  
83 generic climate states will not work properly. Indeed, fixed points have different time scales and  
84 phase-space directions with respect to a generic point, and thus call for a tailored treatment.

85 In the rest of the study, we compute the persistence and local dimension of tropical cyclones,  
86 and use these to outline a strategy to improve their numerical simulation.

### 87 **III. OBSERVABLES FOR CYCLONE DYNAMICS**

88 The cyclone historical data are the "best track data" from the Atlantic HURDAT2 database<sup>19</sup>,  
89 developed by the National Hurricane Center. This database provides, amongst other variables,  
90 the location of tropical cyclones, their maximum winds, central pressure and categorisation. The  
91 values are obtained as a post-storm analysis of all available data, collected both remotely and in-  
92 situ. We specifically consider separately hurricanes (HU), tropical storms (TS) and post-tropical  
93 cyclones associated with an extratropical transition (EX). We further use instantaneous potential  
94 vorticity (PV) at 500 hPa and sea-level pressure (SLP) data from ECMWF’s ERA5 reanalysis<sup>20</sup>.

95 For both datasets we make use of 6-hourly data; the ERA5 data is retrieved at a horizontal resolu-  
96 tion of  $0.25^\circ$ .

97 Our analysis includes all tropical cyclones classified in HURDAT2 from 2010 to 2020 included.  
98 We use semi-Lagrangian observables, i.e. we select a horizontal domain around the tropical cy-  
99 cloe location, of size  $\sim 1200 \times 1200$  km ( $41 \times 41$  grid points in ERA5). The choice of SLP is  
100 motivated by its widespread use in hurricane tracking<sup>21</sup> and the fact that it is a first approximation  
101 of the horizontal velocity streamfunction. The PV is often used in the study of tropical cyclones  
102 and relates to their intensification and symmetry structure<sup>22,23</sup>, and takes explicitly into account  
103 the strength of the cyclones' warm core. Indeed, PV may be viewed as a metric of latent heat  
104 release and therefore of the intensity of the diabatic processes taking place in the tropical cyclones  
105 (formation of clouds, solid and liquid precipitation)<sup>24,25</sup>. We specifically select mid-level PV,  
106 following for example<sup>26,27</sup>. As control parameter we chose the maximum winds from HURDAT2,  
107 since this quantity can be directly connected to the economic loss caused by tropical cyclones<sup>28</sup>.

#### 108 **IV. A DYNAMICAL SYSTEMS VIEW OF TROPICAL CYCLONES**

109 We follow tropical cyclones in phase space as states of a chaotic, high-dimensional dynamical  
110 system. Each instantaneous state of the cyclone, as represented by a given atmospheric variable,  
111 corresponds to a point in a reduced phase space (namely a special Poincaré section). We sample  
112 these states at discrete points  $i$ , determined by the temporal resolution of the HURDAT2 data,  
113 that is every 6h or whenever the HURDAT2 database displays a cyclone landfall. Our aim is  
114 to diagnose the dynamical properties of the instantaneous (in time) and local (in phase-space)  
115 states of the cyclone, as represented by the chosen atmospheric variable and geographical domain  
116 (physical space in Fig. 1). To do so, we leverage two metrics issuing from the combination of  
117 extreme value theory with Poincaré recurrences<sup>29-31</sup>. We consider the ensemble  $\{X_i\}$ , which in our  
118 analysis are SLP or PV maps of all timesteps for all tropical cyclones in our dataset, always centred  
119 on the cyclones' location. We further consider a state of interest  $\zeta$ , which would correspond to a  
120 single SLP or PV map drawn from this dataset. We then define logarithmic returns as:

$$121 \quad g(X_i, \zeta) = -\log[\text{dist}(X_i, \zeta)] \quad (1)$$

122 Here, *dist* is the Euclidean distance between pairs of SLP or PV maps, but more generally it can  
123 be any distance function between two vectors which tends to zero as the two vectors increasingly

124 resemble each other. We thus have a time series  $g$  of logarithmic returns which is large at times  
 125 when  $X_i$  is close to  $\zeta$ .

126 We next define exceedances as  $u(\zeta) = g(X_i, \zeta) - s(q, \zeta) \forall g(X_i, \zeta_x) > s(q, \zeta)$ , where  $s(q, \zeta)$  is a  
 127 high threshold corresponding to the  $q$ th quantile of  $g(X_i, \zeta)$ . These are effectively the previously-  
 128 mentioned Poincaré recurrences, for the chosen state  $\zeta$  (phase space in Fig. 1). The Freitas-  
 129 Freitas-Todd theorem<sup>29,30</sup> states that the cumulative probability distribution  $F(u, \zeta)$  is approxi-  
 130 mated by the exponential member of the Generalised Pareto Distribution. We thus have that:

$$131 \quad F(u, \zeta) \simeq \exp \left[ -\vartheta(\zeta) \frac{u(\zeta)}{\sigma(\zeta)} \right] \quad (2)$$

132 The parameters  $s(q, \zeta)$ , namely the threshold, and  $\sigma$ , namely the scale parameter of the Gener-  
 133 alised Pareto Distribution, depend on the chosen state  $\zeta$ , while  $\vartheta$  is the so-called extremal index,  
 134 namely a measure of clustering<sup>32</sup>. We estimate it here using the Süveges Estimator<sup>33</sup>.

135 From the above, we can define two dynamical systems metrics: local dimension ( $d$ ) and persis-  
 136 tence ( $\theta^{-1}$ ). The local dimension is given by  $d(\zeta) = 1/\sigma(\zeta)$ , with  $0 \leq d \leq +\infty$ . When  $X_i$  contains  
 137 all the variables of the system, the estimation of  $d$  based on extreme value theory has a number of  
 138 advantages over traditional methods (e.g. the box counting algorithm<sup>34</sup>). First, it does not require  
 139 to estimate the volume of different sets in scale-space: the selection of  $s(q)$  based on the quantile  
 140 provides a selection of different thresholds  $s$  which depends on the recurrence rate around the point  
 141  $\zeta$ . Moreover, it does not require the a-priori selection of the maximum embedding dimension, as  
 142 the observable  $g$  is always a univariate time-series. Even when  $X_i$  does not contain all variables  
 143 of the system, the estimation of  $d$  through extreme value theory is still a powerful tool to compare  
 144 different states of high-dimensional chaotic systems<sup>35</sup>.

145 The persistence of the state  $\zeta$  is measured via the extremal index  $0 < \vartheta(\zeta) < 1$ . We define the  
 146 inverse of the average residence time of trajectories around  $\zeta$  as:  $\theta(\zeta) = \vartheta(\zeta)/\Delta t$ , with  $\Delta t$  being  
 147 the timestep of the underlying data (here 6 hours). Since the extremal index is non-dimensional,  
 148  $\theta(\zeta)$  has units of frequency.  $\theta^{-1}$  is then a measure of persistence. If  $\zeta$  is a fixed point of the  
 149 attractor  $\theta(\zeta) = 0$ . For a trajectory that leaves the neighborhood of  $\zeta$  at the next time iteration,  
 150  $\theta = 1$ . A caveat of our approach is that our dataset is constructed from a sequence of cyclones  
 151 which is not continuous in space-time. This may introduce a bias in our calculation of  $\theta$  if the final  
 152 state of a cyclone is a recurrence of the initial state of the following cyclone. This is highly unlikely  
 153 due to the very different nature of the growth versus weakening stages of tropical cyclones. We  
 154 further note that this does not affect the computation of  $d$ , which is insensitive to time reshuffling.

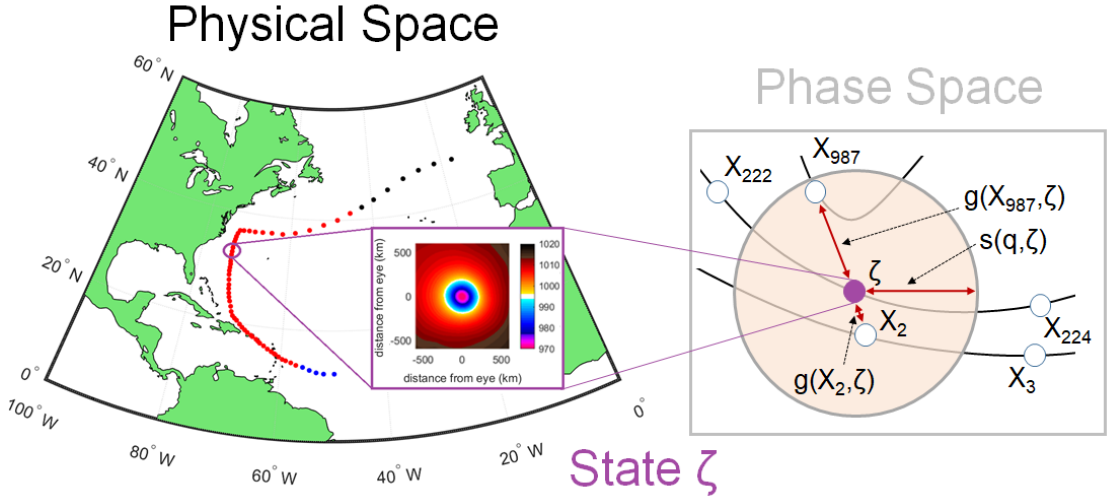


FIG. 1. Schematic of the computation of the dynamical systems metrics for an instantaneous state of a tropical cyclone. We take a snapshot of the cyclone in physical space (black quadrant), in this example a latitude-longitude map of sea-level pressure, which corresponds to state  $\zeta$  in our reduced phase space. The right hand side panel shows the discrete sampling of the phase-space at points  $X_i$  (white circles). The shaded circle is a 2D representation of the hyper-sphere determined by the high threshold  $s(q, \zeta)$ , which defines recurrences. The logarithmic distances between measurements defined by  $g(X_i, \zeta)$  are marked by double-headed arrows. For all points within the hyper-sphere,  $g(X_i, \zeta) > s(q, \zeta)$  holds. In the schematic, only two measurements satisfy this condition (adapted from<sup>14</sup>).

155 While the derivation of  $d$  and  $\theta^{-1}$  may seem very abstract, the two metrics can be related to  
 156 the properties of the tropical cyclones.  $d$  is a proxy for the active number of degrees of freedom  
 157 of the cyclones' instantaneous states. On the other hand,  $\theta^{-1}$  measures the persistence of such  
 158 states and is related to the dominant time scale of the dynamics (the Lyapunov exponent<sup>36</sup>). Both  
 159 these quantities are known to be connected to the dynamical (Kolmogorov Sinai) entropy since the  
 160 seminal work of Young<sup>37</sup>.

## 161 V. DYNAMICAL PROPERTIES OF TROPICAL CYCLONES: COLLAPSE OF 162 DEGREES OF FREEDOM AND PERSISTENCE IN INTENSE STORMS

163 Figure 2a, b shows the values of dimension  $d$  and inverse persistence  $\theta$  computed on SLP and  
 164 500 hPa PV, with maximum winds in colours. The two local dimensions show different ranges,



165 with  $d_{SLP} < 30$  and  $d_{PV}$  attaining higher values. This reflects the richer spatial structure of the  
 166 PV field at multiple spatial scales, which reflect both convective and larger-scale aspects of the  
 167 cyclones. SLP instead reflects the synoptic-scale structures ( $\sim 10^3$  km). The range of local dimen-  
 168 sions found is relatively low compared to the number of grid-points used, which is  $41 \times 41$ . This  
 169 means that the majority of the degrees of freedom are frozen when we follow coherent convective  
 170 phenomena such as tropical cyclones. Moreover, the lag-0 cross-correlation coefficient between  
 171  $d_{SLP}$  and  $d_{PV}$  is 0.23, suggesting that the two variables carry different information. The persistence  
 172 range is also different for SLP and PV, with  $0.1 < \theta_{SLP} < 1$  and  $0.3 < \theta_{PV} < 0.8$ . In units of time,  
 173 these values indicate an SLP persistence between 6 and 60 hours and a PV persistence between  
 174 7.5 and 20 hours. A timescale of 1–2.5 days is consistent with the synoptic-scale intensification of  
 175 a cyclone, while timescales of a few hours to a day are consistent with changes in the convective  
 176 structure of a cyclone. The lag-0 cross-correlation coefficient between  $\theta_{SLP}$  and  $\theta_{PV}$  is 0.02, even  
 177 lower than for  $d$ , again suggesting that the two carry little mutual information.

178

179 We now connect the values of  $d$  and  $\theta$  for SLP and PV to the underlying physics of the storms  
 180 using the maximum wind speed. For SLP (Figure 2a) we note a strong dependence of  $\theta$  on the  
 181 maximum winds. Low to moderate winds are associated with high  $\theta$ , while stronger winds cor-  
 182 respond to lower  $\theta$ . A weaker relation holds for  $d_{SLP}$  and maximum winds. For PV (Figure 2b),  
 183 strong winds match low  $d$  values and intermediate-to-high  $\theta$  values. Thus, SLP suggests that in-  
 184 tense cyclones correspond to persistent states, while PV that they display a low local dimension  
 185 and intermediate-to-low persistence. Looking at the scatterplots and PDFs of the two dynamical  
 186 systems metrics conditioned on the HURDAT2 cyclone classification (Figure 2c, d), provides a  
 187 picture consistent with the above. For SLP, HU and EX display a markedly higher persistence  
 188 than TS. For PV, HU display a lower dimension and lower persistence than both TS and EX. The  
 189 medians of all PDFs are significantly different at the 1% level under a Wilcoxon ranksum test,  
 190 except for  $d_{SLP}$  for HU and EX (not shown). We interpret these dynamical system properties  
 191 as follows. When the storms produce strong winds and diabatic phenomena (HU with high PV  
 192 values and strong precipitation), the convective-scale dynamics collapses to an object with few  
 193 degrees of freedom (low  $d_{PV}$ ), yet low persistence (high  $\theta_{PV}$ ). Nonetheless, the synoptic-scale  
 194 HU field is highly persistent (low  $\theta_{SLP}$ ), with values comparable to those of EX. SLP reflects a  
 195 quasi-symmetrical horizontal cyclonic structure, which for both HU and EX is characteristic of  
 196 the cyclone over an extended period of time. Weaker TS likely do not have a coherent cyclonic

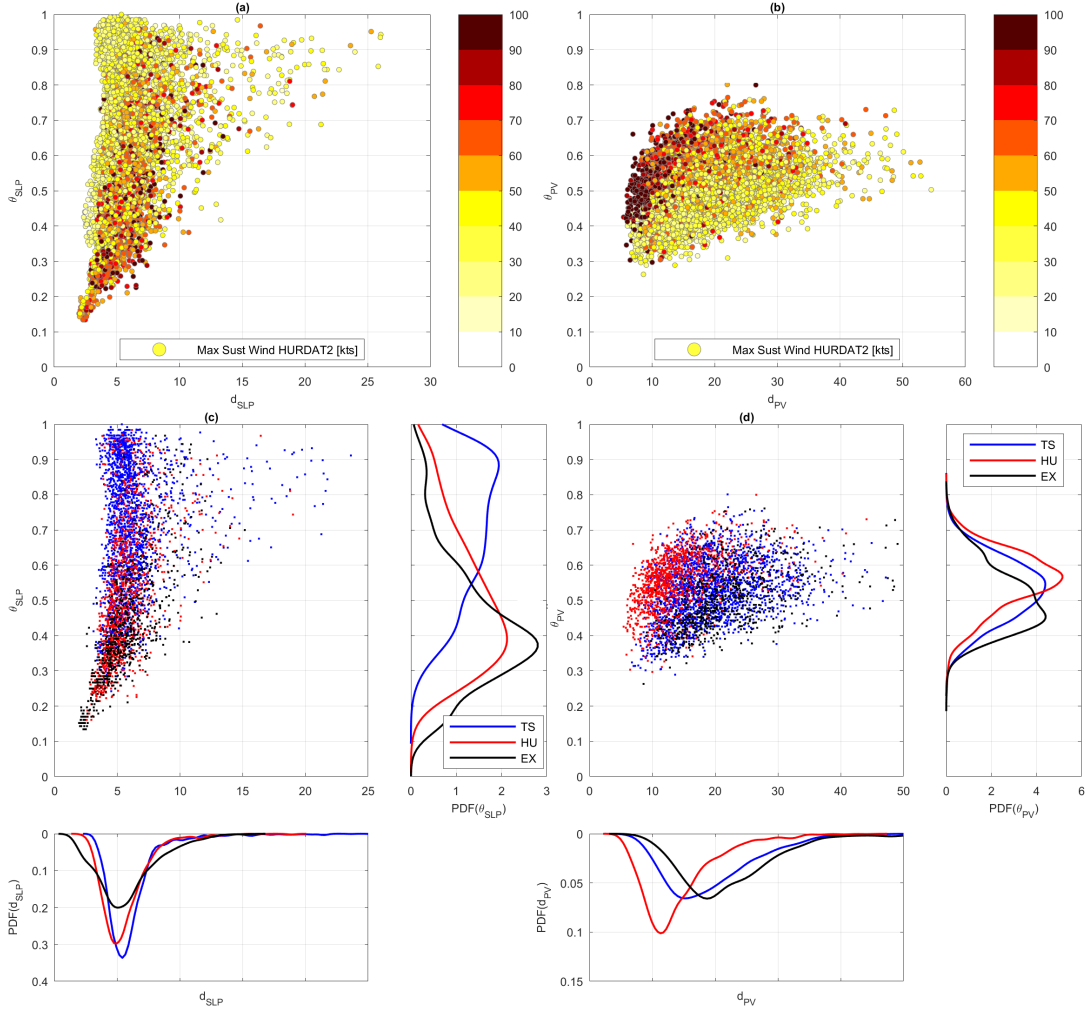


FIG. 2. Dimension  $d$  and inverse persistence  $\theta$  of tropical cyclones, calculated on sea-level pressure (SLP; a,c) and 500 hPa potential vorticity (PV; b, d). The colourscales show maximum wind (a, b) and cyclone classification (c,d, see legend). Side panels show the corresponding PDFs. TS: Tropical Storm; HU: Hurricane; EX: Extratropical cyclones.

197 core throughout their life cycle, as reflected in the high values of  $\theta_{SLP}$ . In the dynamical systems  
 198 framework, the SLP and PV properties of the hurricanes may be interpreted as the signature of an  
 199 unstable fixed point in the underlying phase-space, i.e. a state of the dynamics where the tempo-  
 200 ral and spatial scales are deformed. However, the different relationships between the dynamical  
 201 indicators of SLP and PV with intense hurricanes make it difficult to understand the nature of the  
 202 unstable fixed point (saddle or spiral type).

203 The mean SLP and PV footprints of the system are qualitatively similar across all three cy-

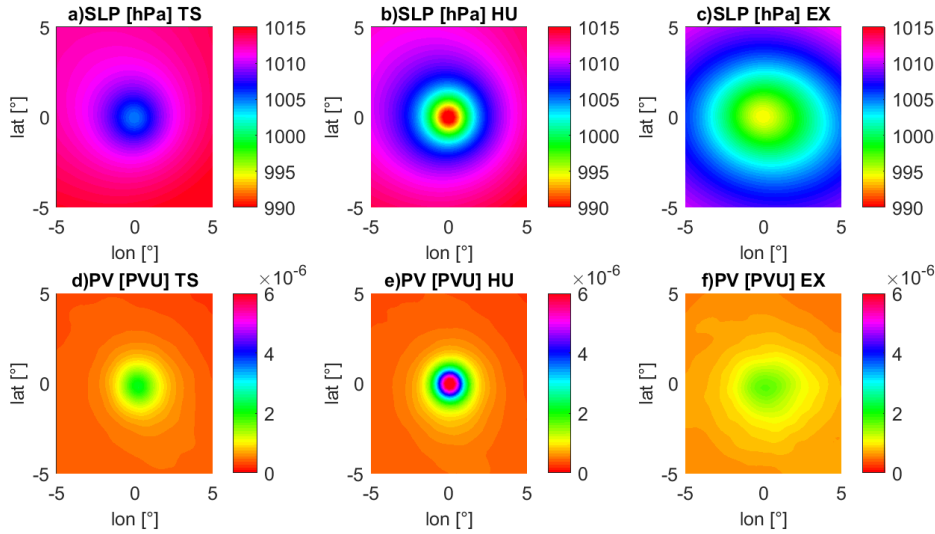


FIG. 3. Average sea-level pressure (SLP, hPa, a–c) and 500 hPa potential vorticity (PV, PVU, d–f) maps conditioned on cyclone classification (TS: Tropical Storm, a,d; HU: Hurricanes, b, e; EX: Extratropical cyclones, c,f).

clone categories (Fig. 3), although EX show a larger spatial scale than both TS and HU. In all three cases, the structures are roughly axisymmetric, showing that the EX cyclones included in HURDAT2 still retain tropical-like characteristics. Clearer differences emerge when looking at the standard deviation of the SLP and PV maps, computed at each gridpoint over all maps included in our analysis (Fig. 4). Here, HU and TS show qualitatively similar, axisymmetric structures, while EX show a clear meridional asymmetry in SLP and a less marked zonal asymmetry in PV. Notwithstanding the broad similarity in mean structure between three cyclone categories, the dynamical systems metrics are nonetheless able to differentiate their characteristics. This suggests that they sample from the systems' dynamic variability and other subtle differences that do not emerge from the composite maps, such as the evolution of the system's mean structure during the different phases of its lifecycle.

215

## 216 VI. DYNAMICAL SYSTEMS METRICS AND RAPID INTENSIFICATION

217 We now investigate whether the same dynamical systems framework can be used to investigate  
 218 rapid intensification. Rapid intensification occurs when a tropical cyclone gains strength dramati-

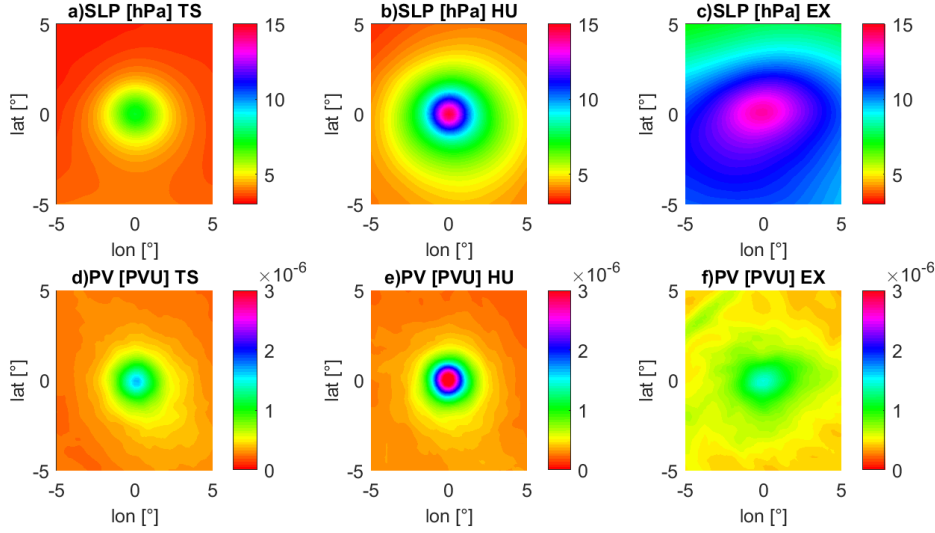


FIG. 4. Same as in Fig. 3, but for the standard deviation of the maps.

219 cally in a short period of time<sup>38</sup>. This phenomenon, difficult to explain from a theoretical point of  
 220 view<sup>39,40</sup>, results in an enhancement of the destructiveness potential of the cyclone and in a lower  
 221 predictability of its trajectory<sup>41</sup>. Rapid intensification is usually quantified using the increment  
 222  $\Delta v$  of maximum winds over 24h. According to this definition, a cyclone is rapidly intensifying  
 223 (resp. weakening) when  $\Delta v > 35$  kts (resp.  $\Delta v < -35$  kts). In phase space, rapid changes of the  
 224 dynamics correspond to approaching unstable fixed points or event to tipping to other basin of  
 225 attraction<sup>42,43</sup>. Our working hypothesis is that variations in the dynamical systems metrics may  
 226 be able to track these transitions. Figures 5 and 6 show the values of (a)  $\Delta d$  and (b)  $\Delta \theta$  associ-  
 227 ated with the rapid intensification or weakening of the cyclones. The  $\Delta$  are again computed over  
 228 a period of 24 hours. Lateral panels show the PDFs of  $\Delta d$  and (b)  $\Delta \theta$  conditioned on the rapid  
 229 weakening or intensification. In both Figures 5 and 6 the medians of all PDFs for rapid weakening  
 230 or intensification are significantly different at the 1% level under a Wilcoxon ranksum test, except  
 231 for  $\Delta \theta_{PV}$ . Rapid intensification is associated with a clear decrease of  $\theta_{SLP}$  and a weak decrease  
 232 of  $d_{PV}$ . In other words, there is a large coherence of the dynamics of the cyclones tracked by  
 233 the increased persistence of the SLP. This hints to the fact that dynamics approaches an unstable  
 234 fixed point<sup>44</sup>. This is accompanied by a decrease of the degrees of freedom in PV, again consistent  
 235 with approaching an unstable fixed point of the dynamics. The rapid weakening displays instead  
 236 a decreased SLP persistence and a marked increase in  $d_{PV}$ . We interpret this as a departure from  
 237 the neighbourhood of a fixed point towards the main basin of attraction of the tropical atmospheric

238 dynamics.

## 239 **VII. IMPLICATIONS OF THE RESULTS FOR THE NUMERICAL SIMULATION OF** 240 **HURRICANES**

241 From a dynamical systems viewpoint, high persistence and low dimensional states are found at  
242 unstable fixed points of the dynamics. Properties such as the local entropy, persistence and number  
243 of active degrees of freedom are greatly affected in the proximity of unstable fixed points, coincid-  
244 ing with deformation of the typical spatial and temporal lengths of the dynamics. This phase-space  
245 phenomenon is reminiscent of what is observed in physical space, when approaching singularities  
246 of turbulent dynamics with well-identified front-like or spiral-like coherent structures accompany-  
247 ing a point of very strong dissipation<sup>45,46</sup>. Although dynamics at fixed points can be fully resolved  
248 when having a perfect model of the underlying dynamics, unstable fixed points are by nature frag-  
249 ile to noise or approximation in the sense that any perturbation will escape following unstable  
250 directions. This may explain from a dynamical systems viewpoint why it is so difficult to obtain  
251 an adequate representation of intense tropical cyclones in climate models. Parameterisations are  
252 devised for typical states of tropical dynamics (disorganized storms), but not specifically for the  
253 organized states of the most intense tropical cyclones. Hurricanes would then be analogous to dis-  
254 sipative singularities of turbulent flows<sup>45</sup>, or *black holes* of the atmospheric dynamics<sup>46</sup>. In these  
255 cases, the physics is far removed from that of the average states of the system, such that adaptive  
256 scaling laws and targeted parametrizations are needed. Thus, the computation of the dynamical  
257 systems metrics could support the development of hurricane-specific parameterizations.

258 As a caveat, we underline that our semi-Lagrangian approach does not allow to relate the  
259 present results to the predictability of the trajectories of the tropical cyclones examined in this  
260 study, unlike the Eulerian approach applied to extra-tropical motions in<sup>9-11</sup>. Furthermore, here  
261 we have used the ERA5 dataset which has a fair but not highly-resolved representation of the  
262 convective scales of hurricane dynamics.

263 To conclude, we have shown that the physical characteristics of tropical cyclones may be un-  
264 derstood in terms of dynamical systems metrics, which are capable of singling out peculiar states  
265 of the dynamics. Our results support the idea that cyclones can be understood as being reached  
266 along specific directions of the dynamics, consistent with instanton theory<sup>47</sup> and the notion of  
267 melancholia states<sup>48</sup>. This perspective opens intriguing possibilities, including the use of impor-

268 tance sampling algorithms<sup>49</sup> to select simulations which approach the hurricanes' fixed points as  
269 detected from the dimension–persistence analysis in the phase space.

270

## 271 **VIII. ACKNOWLEDGMENTS**

272 The authors acknowledge the support of the INSU-CNRS-LEFE-MANU grant (project DINCLIC),  
273 as well as the grant ANR-19-ERC7-0003 (BOREAS). This work has received support from  
274 the European Union's Horizon 2020 research and innovation programme (Grant agreement No.  
275 101003469, XAIDA) and from the European Research Council (ERC) under the European Union's  
276 Horizon 2020 research and innovation programme (Grant agreement No. 948309, CENÆ project).  
277 B. Dubrulle was partly supported by the ANR, project EXPLOIT (grant agreement No. ANR-16-  
278 CE06-0006-01).

## 279 **IX. DATA AVAILABILITY**

280 ERA5 data are available on the C3S Climate Data Store on regular latitude-longitude grids  
281 at 0.25° x 0.25° resolution at <https://cds.climate.copernicus.eu/#!/home>, accessed on  
282 2022-02-23

283

284 HURDAT2 is a database provided by NOAA and freely available at [https://www.aoml.  
285 noaa.gov/hrd/hurdat/Data\\_Storm.html](https://www.aoml.noaa.gov/hrd/hurdat/Data_Storm.html), accessed on 2022-02-23

## 286 **REFERENCES**

287 <sup>1</sup>A. B. Smith and R. W. Katz, “Us billion-dollar weather and climate disasters: data sources,  
288 trends, accuracy and biases,” *Natural hazards* **67**, 387–410 (2013).

289 <sup>2</sup>A. Grinsted, P. Ditlevsen, and J. H. Christensen, “Normalized us hurricane damage estimates  
290 using area of total destruction, 1900- 2018,” *Proceedings of the National Academy of Sciences*  
291 **116**, 23942–23946 (2019).

292 <sup>3</sup>E. K. Chang and Y. Guo, “Is the number of north atlantic tropical cyclones significantly under-  
293 estimated prior to the availability of satellite observations?” *Geophysical Research Letters* **34**  
294 (2007).

- 295 <sup>4</sup>J. Kossin, T. Hall, T. Knutson, K. Kunkel, R. Trapp, D. Waliser, and M. Wehner, “Extreme  
296 storms,” (2017).
- 297 <sup>5</sup>M. J. Roberts, J. Camp, J. Seddon, P. L. Vidale, K. Hodges, B. Vannière, J. Mecking, R. Haarsma,  
298 A. Bellucci, E. Scoccimarro, *et al.*, “Projected future changes in tropical cyclones using the  
299 cmip6 highresmip multimodel ensemble,” *Geophysical Research Letters* **47**, e2020GL088662  
300 (2020).
- 301 <sup>6</sup>E. N. Lorenz, “Can chaos and intransitivity lead to interannual variability?” *Tellus A* **42**, 378–  
302 389 (1990).
- 303 <sup>7</sup>S. Schubert and V. Lucarini, “Covariant Lyapunov vectors of a quasi-geostrophic baroclinic  
304 model: analysis of instabilities and feedbacks,” *Quarterly Journal of the Royal Meteorological*  
305 *Society* **141**, 3040–3055 (2015).
- 306 <sup>8</sup>C. J. Muller and D. M. Romps, “Acceleration of tropical cyclogenesis by self-aggregation feed-  
307 backs,” *Proceedings of the National Academy of Sciences* **115**, 2930–2935 (2018).
- 308 <sup>9</sup>D. Faranda, G. Messori, and P. Yiou, “Dynamical proxies of north atlantic predictability and  
309 extremes,” *Scientific reports* **7**, 41278 (2017).
- 310 <sup>10</sup>G. Messori, R. Caballero, and D. Faranda, “A dynamical systems approach to studying midlat-  
311 itude weather extremes,” *Geophysical Research Letters* **44**, 3346–3354 (2017).
- 312 <sup>11</sup>A. Hochman, P. Alpert, T. Harpaz, H. Saaroni, and G. Messori, “A new dynamical systems  
313 perspective on atmospheric predictability: Eastern mediterranean weather regimes as a case  
314 study,” *Science advances* **5**, eaau0936 (2019).
- 315 <sup>12</sup>A. Hochman, G. Messori, J. F. Quinting, J. G. Pinto, and C. M. Grams, “Do atlantic-european  
316 weather regimes physically exist?” *Geophysical Research Letters* **48**, e2021GL095574 (2021).
- 317 <sup>13</sup>M. Brunetti, J. Kasparian, and C. V  rard, “Co-existing climate attractors in a coupled aqua-  
318 planet,” *Climate Dynamics* **53**, 6293–6308 (2019).
- 319 <sup>14</sup>G. Messori and D. Faranda, “Technical note: Characterising and comparing different palaeocli-  
320 mates with dynamical systems theory,” *Climate of the Past Discussions* (2020).
- 321 <sup>15</sup>A. Gualandi, J.-P. Avouac, S. Michel, and D. Faranda, “The predictable chaos of slow earth-  
322 quakes,” *Science advances* **6**, eaaz5548 (2020).
- 323 <sup>16</sup>D. Faranda, M. C. Alvarez-Castro, G. Messori, D. Rodrigues, and P. Yiou, “The hammam effect  
324 or how a warm ocean enhances large scale atmospheric predictability,” *Nature communications*  
325 **10**, 1–7 (2019).
- 326 <sup>17</sup>A. Crisanti, M. Falcioni, A. Vulpiani, and G. Paladin, “Lagrangian chaos: transport, mixing and

diffusion in fluids,” *La Rivista del Nuovo Cimento* (1978-1999) **14**, 1–80 (1991).

<sup>18</sup>A. Vulpiani, *Chaos: from simple models to complex systems*, Vol. 17 (World Scientific, 2010).

<sup>19</sup>C. W. Landsea and J. L. Franklin, “Atlantic hurricane database uncertainty and presentation of a new database format,” *Monthly Weather Review* **141**, 3576–3592 (2013).

<sup>20</sup>H. Hersbach, B. Bell, P. Berrisford, S. Hirahara, A. Horányi, J. Muñoz-Sabater, J. Nicolas, C. Peubey, R. Radu, D. Schepers, *et al.*, “The era5 global reanalysis,” *Quarterly Journal of the Royal Meteorological Society* **146**, 1999–2049 (2020).

<sup>21</sup>J. B. Elsner, “Tracking hurricanes,” *Bulletin of the American Meteorological Society* **84**, 353–356 (2003).

<sup>22</sup>J. D. Möller and M. T. Montgomery, “Tropical cyclone evolution via potential vorticity anomalies in a three-dimensional balance model,” *Journal of the atmospheric sciences* **57**, 3366–3387 (2000).

<sup>23</sup>L. J. Shapiro, “Potential vorticity asymmetries and tropical cyclone evolution in a moist three-layer model,” *Journal of the atmospheric sciences* **57**, 3645–3662 (2000).

<sup>24</sup>L. J. Shapiro and J. L. Franklin, “Potential vorticity in hurricane gloria,” *Monthly weather review* **123**, 1465–1475 (1995).

<sup>25</sup>S. A. Hausman, K. V. Ooyama, and W. H. Schubert, “Potential vorticity structure of simulated hurricanes,” *Journal of the atmospheric sciences* **63**, 87–108 (2006).

<sup>26</sup>K. Tory, N. Davidson, and M. Montgomery, “Prediction and diagnosis of tropical cyclone formation in an nwp system. part iii: Diagnosis of developing and nondeveloping storms,” *Journal of the atmospheric sciences* **64**, 3195–3213 (2007).

<sup>27</sup>T.-Y. Lee, C.-C. Wu, and R. Rios-Berrios, “The role of low-level flow direction on tropical cyclone intensity changes in a moderate-sheared environment,” *Journal of the Atmospheric Sciences* **78**, 2859–2877 (2021).

<sup>28</sup>A. R. Zhai and J. H. Jiang, “Dependence of us hurricane economic loss on maximum wind speed and storm size,” *Environmental Research Letters* **9**, 064019 (2014).

<sup>29</sup>A. C. M. Freitas, J. M. Freitas, and M. Todd, “Hitting time statistics and extreme value theory,” *Probability Theory and Related Fields* **147**, 675–710 (2010).

<sup>30</sup>V. Lucarini, D. Faranda, and J. Wouters, “Universal behaviour of extreme value statistics for selected observables of dynamical systems,” *Journal of statistical physics* **147**, 63–73 (2012).

<sup>31</sup>V. Lucarini, D. Faranda, J. M. M. de Freitas, M. Holland, T. Kuna, M. Nicol, M. Todd, S. Vaienti, *et al.*, *Extremes and recurrence in dynamical systems* (John Wiley & Sons, 2016).



- 359 <sup>32</sup>N. R. Moloney, D. Faranda, and Y. Sato, “An overview of the extremal index,” *Chaos: An*  
360 *Interdisciplinary Journal of Nonlinear Science* **29**, 022101 (2019).
- 361 <sup>33</sup>M. Süveges, “Likelihood estimation of the extremal index,” *Extremes* **10**, 41–55 (2007).
- 362 <sup>34</sup>N. Sarkar and B. B. Chaudhuri, “An efficient differential box-counting approach to compute  
363 fractal dimension of image,” *IEEE Transactions on systems, man, and cybernetics* **24**, 115–120  
364 (1994).
- 365 <sup>35</sup>F. M. E. Pons, G. Messori, M. C. Alvarez-Castro, and D. Faranda, “Sampling hyperspheres via  
366 extreme value theory: implications for measuring attractor dimensions,” *Journal of statistical*  
367 *physics* **179**, 1698–1717 (2020).
- 368 <sup>36</sup>D. Faranda and S. Vaienti, “Correlation dimension and phase space contraction via extreme  
369 value theory,” *Chaos: An Interdisciplinary Journal of Nonlinear Science* **28**, 041103 (2018).
- 370 <sup>37</sup>L.-S. Young, “Dimension, entropy and lyapunov exponents,” *Ergodic theory and dynamical sys-*  
371 *tems* **2**, 109–124 (1982).
- 372 <sup>38</sup>F. Sanders, “Explosive cyclogenesis in the west-central north atlantic ocean, 1981–84. part i:  
373 Composite structure and mean behavior,” *Monthly weather review* **114**, 1781–1794 (1986).
- 374 <sup>39</sup>R. Klein, “Scale-dependent models for atmospheric flows,” *Annual review of fluid mechanics*  
375 **42**, 249–274 (2010).
- 376 <sup>40</sup>A. V. Soloviev, R. Lukas, M. A. Donelan, B. K. Haus, and I. Ginis, “Is the state of the air-  
377 sea interface a factor in rapid intensification and rapid decline of tropical cyclones?” *Journal of*  
378 *Geophysical Research: Oceans* **122**, 10174–10183 (2017).
- 379 <sup>41</sup>C.-Y. Lee, M. K. Tippett, A. H. Sobel, and S. J. Camargo, “Rapid intensification and the bimodal  
380 distribution of tropical cyclone intensity,” *Nature communications* **7**, 1–5 (2016).
- 381 <sup>42</sup>M. Ghil, M. D. Chekroun, and E. Simonnet, “Climate dynamics and fluid mechanics: Natural  
382 variability and related uncertainties,” *Physica D: Nonlinear Phenomena* **237**, 2111–2126 (2008).
- 383 <sup>43</sup>H. A. Dijkstra, *Nonlinear climate dynamics* (Cambridge University Press, 2013).
- 384 <sup>44</sup>L. Dai, D. Vorselen, K. S. Korolev, and J. Gore, “Generic indicators for loss of resilience before  
385 a tipping point leading to population collapse,” *Science* **336**, 1175–1177 (2012).
- 386 <sup>45</sup>E.-W. Saw, D. Kuzzay, D. Faranda, A. Guittonneau, F. Daviaud, C. Wiertel-Gasquet, V. Padilla,  
387 and B. Dubrulle, “Experimental characterization of extreme events of inertial dissipation in a  
388 turbulent swirling flow,” *Nature communications* **7**, 1–8 (2016).
- 389 <sup>46</sup>J. Grover and A. Wittig, “Black hole shadows and invariant phase space structures,” *Physical*  
390 *Review D* **96**, 024045 (2017).

391 <sup>47</sup>F. Bouchet, J. Laurie, and O. Zaboronski, “Langevin dynamics, large deviations and instantons  
392 for the quasi-geostrophic model and two-dimensional euler equations,” *Journal of Statistical*  
393 *Physics* **156**, 1066–1092 (2014).

394 <sup>48</sup>V. Lucarini and T. Bódai, “Edge states in the climate system: exploring global instabilities and  
395 critical transitions,” *Nonlinearity* **30**, R32 (2017).

396 <sup>49</sup>F. Ragone, J. Wouters, and F. Bouchet, “Computation of extreme heat waves in climate models  
397 using a large deviation algorithm,” *Proceedings of the National Academy of Sciences* **115**, 24–29  
398 (2018).

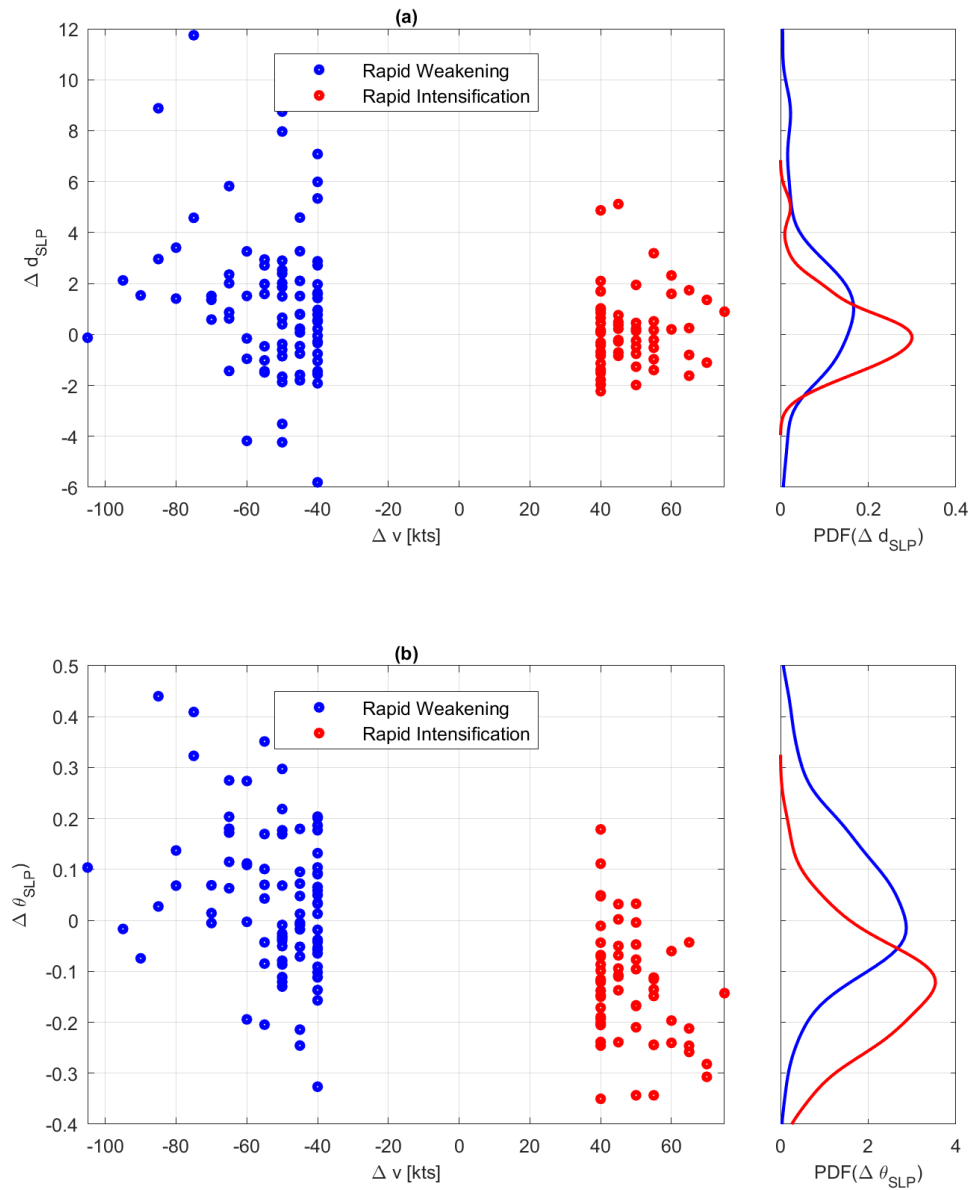


FIG. 5. 24h variation ( $\Delta$ ) of the dimension  $d$  (a) and of the inverse persistence  $\theta$  (b) computed on SLP versus the 24h variation of maximum winds  $v$  for rapidly intensifying (blue) and rapidly weakening (red) cyclones. The side panel shows the corresponding PDFs.

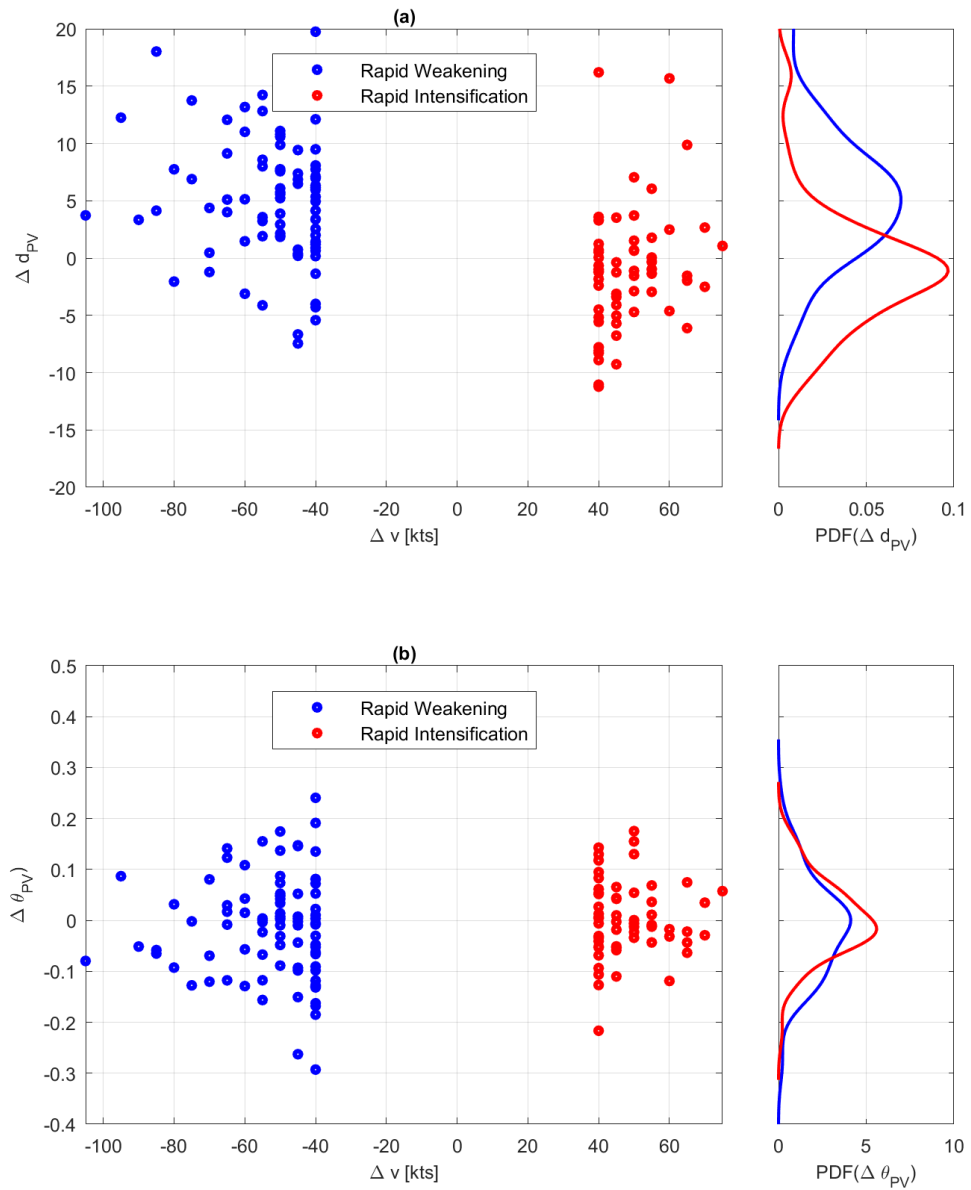


FIG. 6. Same as Fig. 5, but for  $d$  and  $\theta$  computed on PV at 500 hPa.